Hindawi
International Journal of Energy Research
Volume 2024, Article ID 6314966, 13 pages
https://doi.org/10.1155/2024/6314966

Research Article

A Blocking Method for Overload-Dominant Cascading Failures in Power Grid Based on Source and Load Collaborative Regulation

Ji Sun, Jiajun Liu, Yue Liu, Chenjing Li, and Na Zhi

Xi'an University of Technology, School of Electrical Engineering, 58 Yanxiang Road, Xi'an City, Shaanxi Province, China

Correspondence should be addressed to Ji Sun; sunji2021@126.com

Received 19 December 2023; Revised 27 March 2024; Accepted 25 April 2024; Published 18 May 2024

Academic Editor: Olubayo Babatunde

Adjusting generator output and cutting off load can effectively solve the problem of continuous overload and disconnection of power lines caused by power flow transfer. To suppress large-scale power outages caused by overload-dominant cascading failures, a blocking method for overload-dominant cascading failures in the power grid based on source and load collaborative regulation is proposed. The shortest path algorithm was used to identify loads and generators with shorter electrical distances from overloaded lines. Under the premise of meeting the static safety constraints of the power grid, considering the regulation of generator output and the removal of interruptible loads, a multiobjective cascading failure blocking model is established with the minimum overall control cost of the system and the minimum probability coefficient of line failure. Use the NSGA-II algorithm to solve the model and obtain the optimal plan for adjusting generator output and cutting off load. Through example verification, the proposed method can effectively alleviate the phenomenon of line overload, thereby blocking the continuation of overload-dominant cascading failures.

1. Introduction

With the pursuit of economic benefits, the improvement of transmission efficiency, and the integration of large-scale new energy sources in the power grid, the margin for safe operation of the system is gradually shrinking, and the operation mode and power flow distribution of the power grid are becoming more diverse, further increasing the possibility of major power outages. Large-scale power outages are usually caused by cascading failures (CF), which typically manifest as local disturbances such as generator failures and transmission line issues. These small disturbances gradually trigger CF of power grid components through grid connections, leading to malignant cascading reactions [1, 2]. Therefore, it is crucial to quickly and accurately track the development path of CF, as well as develop targeted prevention and control strategies for CF and interruption control in accidents, to ensure the safe operation of the power system and reduce losses from power outages [3, 4].

Cascading failure blocking (CFB) belongs to emergency control, and the main control measures include adjusting generator output (AGO), cutting off load (COL), DC modulation, electrical braking, and fast closing of steam turbine valves [5]. Some of the above control measures are manually operated by operators, while others are automatically triggered by the system. Ideally, these emergency control measures can alleviate real-time issues in the power grid. However, manual operation heavily relies on the operator to choose the appropriate control operation, making it difficult to manually make the correct blocking action in a very short decision-making time. The existing emergency control systems are usually determined offline based on some typical scenarios. These types of emergency control triggered by the system are based on the system's predictions and imagined emergency scenarios through offline research. Their decisions are usually fixed and unchanging. In the face of increasingly complex power grid situations, the limited set of expected accidents is gradually unable to meet the demand [6]. For example, in 2019, an N-1 fault occurred in the northeast power grid of Argentina. The accident investigation report pointed out that after the line was correctly tripped, the power grid company did not update the strategy of the automatic cutting system in advance, and the command to cut off 1200 MW was not issued, resulting

in a chain of subsequent faults and ultimately leading to a major power outage between Argentina and Uruguay. Therefore, it is necessary to study a real-time interlocking fault blocking method that can adapt to different power grid conditions [7].

At present, many scholars have studied the methods for blocking cascading faults. After CF in the power grid, there is a possibility of frequency instability, and it is generally avoided by cutting off a portion of the load. Reference [8] constructed a noncooperative game model with the goal of meeting the operational needs of the power grid and minimizing user losses and solved the optimal solution. In order to more efficiently eliminate line overload and block CF, AGO and COL are usually used in combination [9]. Reference [10] points out that when formulating a CFB scheme, factors such as eliminating line overload and minimizing economic compensation should be considered, and power sensitivity should be used as the evaluation basis for the control of overloaded lines. This type of model generally prevents and controls selected fault modes, ignoring the impact of the current operating state of the power grid on the probability of system component failures. It is difficult to quantify the safety level of the power grid in a reasonable manner, leading to a conservative control scheme. For this reason, many studies have introduced risk assessment theory that takes into account uncertain factors in system operation into chain fault control, providing control schemes that balance safety and economy [11–15]. The CFB model established in reference [12] adds the thermal limit constraint of overload lines, making the model more in line with practical needs. However, the control strategy for CF mentioned above was calculated based on deterministic criteria and did not consider the impact of the current operating state of the power system on the outage probability of power system components. The line failure probability (LFP) is closely related to the operating state, and ignoring this factor may result in the control strategy being too conservative and sacrificing economic efficiency [13]. References [13, 14] established a CFB model considering the probability of transmission line outage. Based on this CFB control model, the control strategy obtained can effectively reduce the LFP within the fault path while driving CF to develop according to the predicted propagation path. This provides an important reference for the defense decision-making of CF. CFB schemes often involve multiple generators and load nodes, and adopting a global traversal search method is obviously not efficient. Therefore, intelligent optimization algorithms are often used. Currently, algorithms with better performance include genetic algorithms and particle swarm optimization algorithms [8, 12–15]. This type of method can relatively quickly solve the optimal solution of the model, but such algorithms may also encounter problems of falling into local optima or having too many iterations when facing solutions with very complex demand solutions. Therefore, it is necessary to preprocess the solution to simplify the optimization problem and reduce computational complexity [14, 15].

With the deepening of research, the modeling of the CFB process is becoming more and more perfect, and equating it to a global optimal problem is currently a relatively mature method [16]. The main problems faced by current modeling methods for CFB are as follows:

(1) In the modeling of CFB models, traditional methods often consider minimizing the cost of AGO and COL as the objective function and rarely consider the impact of AGO and COL on the LFP. They often use one of the transient or steady-state indicators of the power system as a constraint, which may result in some strategies not being optimal. Therefore, a reasonable modeling method is one of the difficulties

(2) In terms of solving the CFB model, when the model is treated as the overall optimal problem, traditional methods will simplify the multiobjective problem into a single objective problem, and the simplification of the problem may make the final solution not optimal. Therefore, efficiently and accurately solving the model is one of the difficulties

This paper proposes a blocking method for overload-dominant cascading failures (ODCF) in power grid based on source and load collaborative regulation, which can effectively alleviate the phenomenon of line overload and suppress the continuation of ODCF. The main contributions of this paper are as follows:

(1) Analyze the development process of ODCF, and use AGO and COL as suppression methods for ODCF. The problem of CFB is equivalent to two parts: selecting the nodes for AGO and COL and calculating the AGO and COL capacity. The above two parts are calculated separately to reduce the calculation amount

(2) By using the shortest path algorithm to identify the load and generator that are electrically close to the overload line, determine the nodes for AGO and COL, and explore the relationship between the number of AGO and COL and the optimality of the scheme

(3) Establish a multiobjective power grid CFB model that minimizes the overall control cost of the system and the LFP. Use the NSGA-II algorithm to solve the model and obtain the optimal plan for AGO and COL, and compare it with three traditional AGO and COL methods to verify the superiority of the proposed method

2. Cascading Failure Blocking Process

CF can be divided into overload-dominant CF, coordination-dominant CF, and structural-dominant CF based on the main driving factors of fault propagation and the nature of critical events. ODCF is caused by the successive overload and disconnection of the line. The slow sequential disconnection phase of ODCF lasts for a long time, during which the

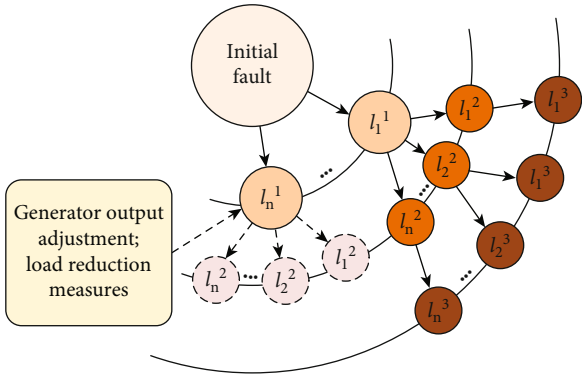

Figure 1: Cascading failure blocking process.

topology of the power grid remains relatively intact and generally does not experience instability. But when the system state continuously deteriorates until a critical event is triggered, it will enter a stage of oscillation and collapse, among which the most common phenomena are disorderly machine cutting, load shedding, and voltage collapse [17, 18].

This type of CF mainly includes slow sequential disconnection stage and fast sequential disconnection stage. Due to the small time level of the fast sequential disconnection stage, it is difficult to block faults during this process, while the time level of the slow sequential disconnection stage is relatively large. Therefore, it is feasible to block faults during this stage. The slow sequential disconnection stage is mainly controlled by the overload phenomenon, while the balance between the source and load is still maintained. At this stage, AGO and COL can effectively alleviate the overload phenomenon of the line, thereby reducing the LFP and blocking the continued development of CF. Therefore, this paper selects AGO and COL control, which can achieve rapid response through switch switching, as a blocking measure. During the occurrence of ODCF, reasonable AGO and COL will effectively block the continued spread of CF [19, 20]. The specific CFB process is shown in Figure 1.

To prevent the development of CF, measures such as AGO and COL need to be taken based on the power grid trend. To ensure the rationality of prevention and control measures and prevent the occurrence of over cutting and less cutting, it is necessary to specify the exact location and control capacity of AGO and COL [21–23]. The CFB control model established in this paper includes AGO and COL location selection and capacity calculation.

3. Cascading Failure Blocking Control Model

3.1. Select the Nodes for AGO and COL. When selecting the nodes for AGO and COL, the shortest path algorithm is used to calculate the distance between the overload line and each load and generator. Sort and filter out the loads and generators that are closer to the overload line as the nodes for AGO and COL.

The shortest path algorithm selected in this paper is the Dijkstra algorithm, which is a classic and mature algorithm for searching for the shortest path in a weighted graph. It adopts a greedy search strategy, gradually searching towards other nodes from the starting point until the target point stops. By using a backtracking array for node backtracking, a shortest feasible path can be found, which is widely used in path planning problems [24, 25]. Figure 2 shows the general operational flowchart of the Dijkstra algorithm.

In order to provide a more intuitive description of the operation process, the Dijkstra algorithm is described using graph theory as follows: Abstract the power system structure diagram as a weighted directed graph, which can be represented as $G = (N, E, W)$. Among them, N is the set of all nodes $n_0, n_1, \cdots, n_n$ in the weighted directed graph, specifically referred to as the bus node in this paper. E is the set of all edges $e_0, e_1, \cdots, e_n$ in the weighted directed graph, specifically referring to the transmission line in this paper. W is the weight set of all edges $w_0, w_1, \cdots, w_n$ in the weighted directed graph, specifically referred to as the line impedance in this paper. Divide the vertex set N into two groups: $N = (S, U)$. The first group is the set of vertices with the shortest path found, represented by S. The initial set of S only contains active nodes. For each shortest path found, the corresponding intermediate node n is added to the set S. The second group is the set of vertices with undetermined shortest paths, represented by U, and the vertices in the second group are added to S in ascending order of the shortest path. In addition, each vertex corresponds to a distance, and the distance of the vertex in S is the shortest path length from the starting point s to the vertex, while the distance of the vertex in U is the shortest path length from the starting point s to the vertex, including only the vertex in S as the middle vertex. The distance between the node and itself is considered as 0. The algorithm steps are as follows:

Step 1. Initially, generate set $S = \{s\}$, set $U = \{\text{other vertices}\}$, and sets S and U complement each other.

Step 2. Select a vertex n with the smallest distance s from set U, add n to set S (this distance is the shortest path from s to n), and record node s as the parent node of node n.

Step 3. Using n as the new intermediate point to consider, modify the distance between each vertex in the U set. If the distance from the source point s to vertex e is shorter than the original distance, modify the distance value of vertex e. The modified distance value is the distance of vertex n plus the weight on the edge, and modify the parent node of node n.

Step 4. Repeat steps 2 and 3 until all vertices are included in the set U.

Step 5. Reverse iteration based on the parent node of the target node to output the shortest path.

The process of finding the nodes for AGO and COL is as follows: using the Dijkstra algorithm to calculate the shortest distance between all generators or loads and the overloaded line, sort the generators or loads based on this distance, and select the node with the highest ranking as the AGO and COL node for this round of scheme.

3.2. Calculation of AGO and COL Capacity

3.2.1. Objective Function. Both the generator and the load need to pay the cost of corrective control when participating in CFB. To minimize the overall control cost of the system, it

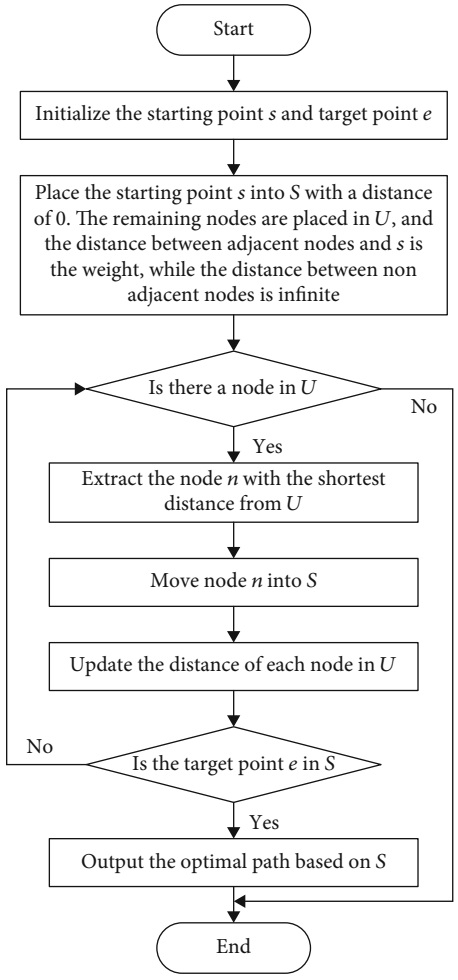

Figure 2: Dijkstra algorithm operation flowchart.

is necessary to synergistically optimize the AGO and COL correction measures. Under the premise of meeting the power flow constraints of the power grid, the objective function f_1 is to minimize the overall control cost of the system, and the calculation formula is shown in

$$f_1 = \min\left(\sum_{i=1}^{N_G} c_{G,i}\Delta P_{G,i} + \sum_{j=1}^{N_L} c_{L,j}\Delta P_{L,j}\right). \quad (1)$$

In the formula, N_G is the number of switchable generator nodes. N_L is the number of load shedding nodes. $c_{G,i}$ is the cutting cost of the i-th generator node, and $c_{L,j}$ is the cutting cost of the j-th load node. $\Delta P_{G,i}$ is the adjustment amount of the i-th generator node. $\Delta P_{L,j}$ is the load shedding amount of the j-th load node.

When formulating a CFB strategy, not only should the control cost be considered, but also the phenomenon of line overload should be eliminated. In the process of CF development, the LFP is one of the important indicators that can reflect the overload situation of the line, and it is also an important criterion for verifying the success of control strategies during the blocking process. The calculation formula for the LFP is shown in equation (2), and the objective function f_2 is to minimize the LFP. The calculation formula is shown in equation (3) [13, 14].

$$p_n = \begin{cases} p_0, & 0 < P \le P_m, \\ p_0 + \dfrac{(1-p_0)(P-P_m)}{(b-1)P_m}, & P_m < P \le bP_m, \\ 1, & P > bP_m. \end{cases} \quad (2)$$

In the formula, p_n is the LPF. p_0 is the probability of hidden faults on the line, which is taken as 0.01 in this paper. P is the transmission power of the line. P_m is the upper limit of line transmission power. b is the multiple of the maximum transmission power, and the value is greater than 1.

To demonstrate the effectiveness of implementing a CFB strategy, another objective function has been established, where f_2 represents the sum of LFP except for the cut-off line. This function reflects the increase and decrease in the LFP after the AGO and COL.

$$f_2 = \min\left(\sum_{i=1}^{N_l} \Delta p_n - (N_l - N_{ol}) * p_0\right). \quad (3)$$

In the formula, N_l is the number of lines, and N_{ol} is the number of lines cut off due to faults.

Establish a multiobjective emergency control model for the power grid that considers the location of AGO and COL, minimizes the overall control cost of the grid, minimizes load shedding, and adjusts the maximum output of the generator.

3.2.2. Constraint Condition

(1) Equation Constraints for Power Flow Equations.

$$P_{Gi}^l - \left(P_{Li} - \sum_{k\in N_i} P_{L.ik}\right) - U_i^l \sum_{j=1}^{n} U_j^l \left(G_{ij}\cos\theta_{ij}^l + B_{ij}\sin\theta_{ij}^l\right) = 0,$$
$$Q_{Gi}^l - \left(Q_{Li} - \sum_{k\in N_i} Q_{L.ik}\right) - U_i^l \sum_{j=1}^{n} U_j^l \left(G_{ij}\sin\theta_{ij}^l - B_{ij}\cos\theta_{ij}^l\right) = 0. \quad (4)$$

In the formula, $Q_{L,ik}$ is the reactive power of the corresponding controllable load generated when $P_{L,ik}$ is cut off. U_i^l is the voltage amplitude of the i-th node during the accident state. P_{Li} and Q_{Li} represent the active and reactive power of the i-th node load. G_{ij} and B_{ij} are the element of the node admittance matrix. θ_{ij}^l is the angle difference between nodes i and j. The meanings of other physical quantities are the same as above.

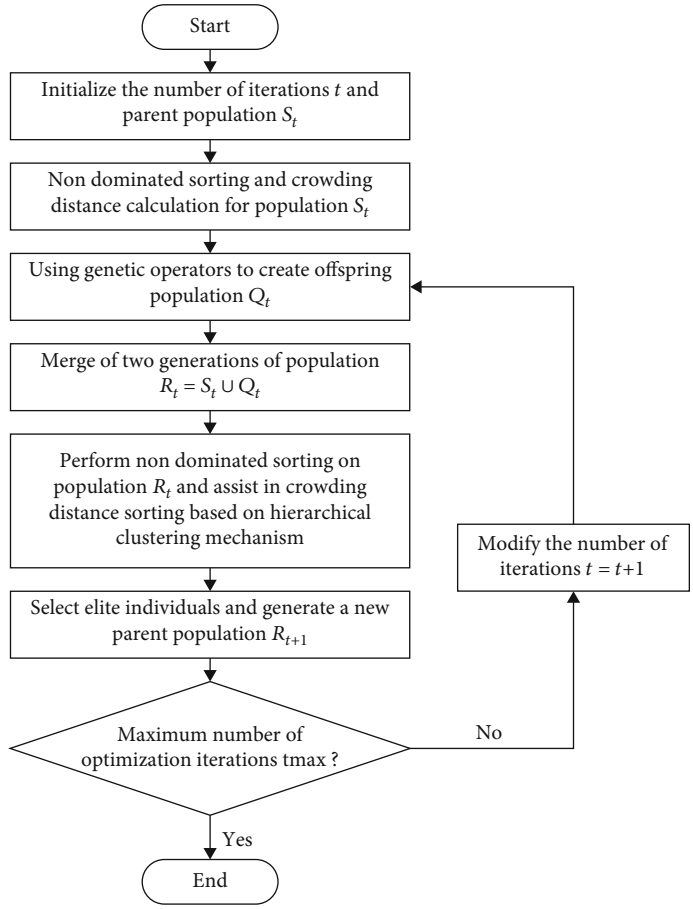

Figure 3: Overall algorithm process.

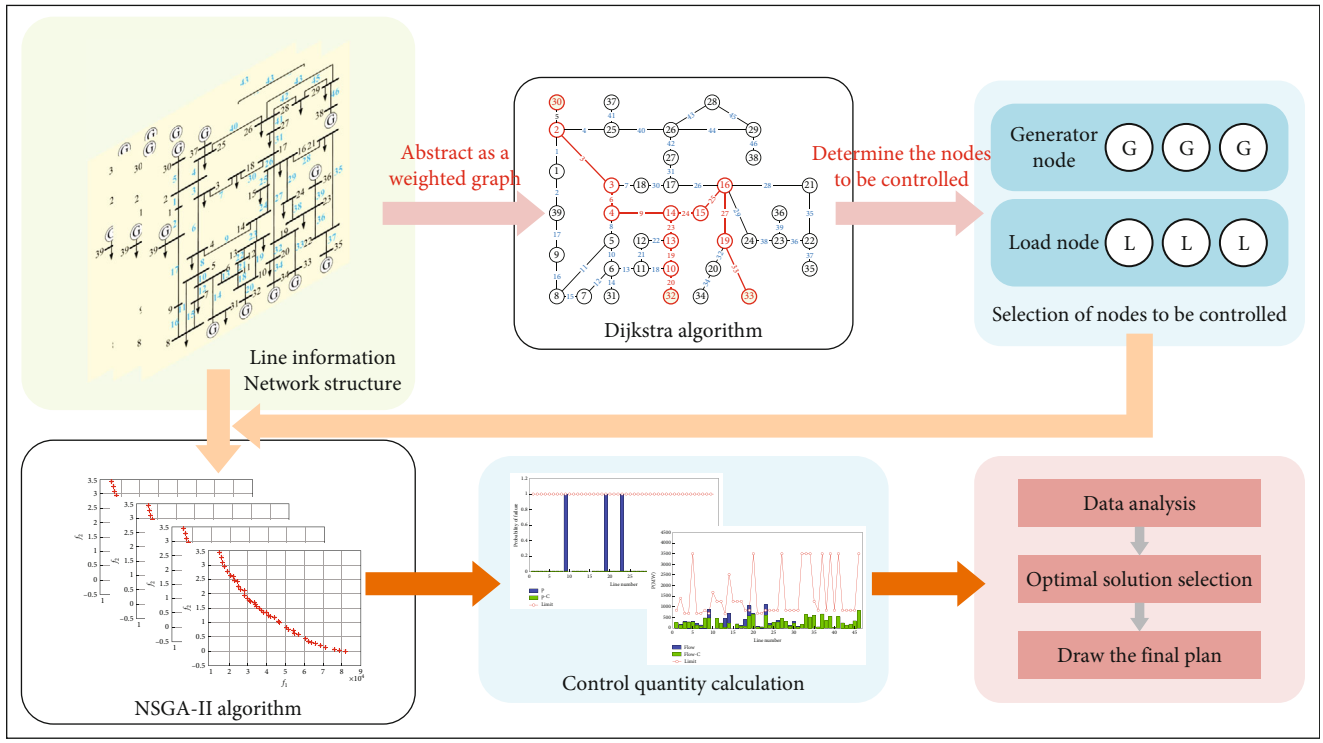

Figure 4: Solution process for the optimal scheme of CFB.

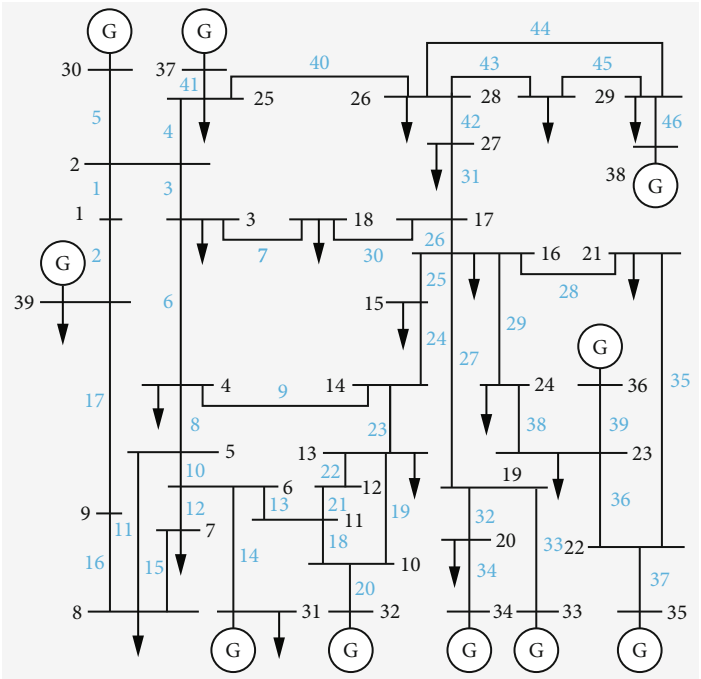

Figure 5: IEEE 39-bus system structure diagram.

(2) Generator Output Constraint.

$$P_{Gi,\min} \le P_{Gi}^{l} \le P_{Gi,\max},$$
$$Q_{Gi,\min} \le Q_{Gi}^{l} \le Q_{Gi,\max}. \tag{5}$$

In the formula, $P_{Gi,\max}$ and $P_{Gi,\min}$ represent the upper and lower limits of the active output of the i-th generator. $Q_{Gi,\max}$ and $Q_{Gi,\min}$ represent the upper and lower limits of the reactive power output of the i-th generator.

(3) Line Power Safety Constraints.

$$P_{ij}^{l} \le P_{ij,\max}. \tag{6}$$

In the formula, P_{ij}^{l} is the transmission power of the line ij during the accident state. $P_{ij,\max}$ is the maximum allowable transmission power of line ij.

(4) Node Voltage Constraint.

$$U_{i,\min} \le U_{i}^{l} \le U_{i,\max}. \tag{7}$$

In the formula, $U_{i,\max}$ and $U_{i,\min}$ represent the upper and lower limits of voltage amplitude at node i, which are 1.05 pu and 0.95 pu.

3.2.3. Solution Algorithm Based on NSGA-II. In the calculation process of AGO and COL control variables, if the global traversal search method is used for calculation, the number of combinations is too large and contains many invalid schemes. To ensure efficient and accurate solution of CFB schemes, this paper uses the NSGA-II algorithm to solve the Pareto frontier of multiobjective optimization models for AGO and COL control and, based on this, selects the overall optimal equilibrium solution. This algorithm is a nondominated sorting genetic algorithm with an elite strategy, which can solve the shortcomings of high complexity and easy loss of optimal solutions in general heuristic algorithms [8, 15]. The solution method based on this algorithm mainly includes the following important steps.

Table 1: The active power output of each generator and the compensation price for unit output changes.

Generator node	Power generation (MW)	Output adjustment compensation price ($·(MW·h)$^{-1}$)	Cutting machine compensation price ($·(MW·h)$^{-1}$)
30	250	6	60
31	677.87	5	50
32	650	9	90
33	632	8	80
34	508	6	60
35	650	9	90
36	560	4	40
37	540	5	50
38	830	7	70
39	1000	7	70

(1) Nondominated Sorting. The NSGA-II algorithm uses nondominated sorting to sort individuals in the population. Nondominated sorting divides individuals into different

Table 2: The active power situation of each load and compensation price for unit load changes.

Load node	Interruptible load capacity (MW)	Load shedding compensation price ($·(MW·h)$^{-1}$)	Load node	Interruptible load capacity (MW)	Load shedding compensation price ($·(MW·h)$^{-1}$)
1	97.6	100	21	274	100
3	322	120	23	247.5	100
4	500	110	24	308.6	100
7	233.8	100	25	224	100
8	522	120	26	139	100
9	6.5	100	27	281	100
12	8.53	100	28	206	100
15	320	100	29	283.5	100
16	329	100	31	9.2	100
18	158	110	39	1104	100
20	680	100			

frontier levels, with the first level containing nondominated solutions, meaning that no other solution can outperform it in all objective functions. This helps to preserve diversity in the population and enables the algorithm to search for various solutions at the Pareto frontier.

(2) Crowding Distance Calculation. The NSGA-II algorithm introduces congestion distance as an indicator to measure the distribution density of individuals in the solution space. Crowding distance represents the local density around an individual, and measuring the distance between an individual and its neighbors helps maintain population diversity. Individuals with larger crowding distances are usually located in sparser areas, while smaller individuals are located in tight areas.

(3) Select Action. NSGA-II uses multiple selection strategies to select the parent individuals of the next generation population. Common selection methods include tournament selection and roulette selection. This paper selects the tournament selection method by randomly selecting two individuals and comparing their nondominated levels and crowding distances to select the winner.

(4) Cross and Mutation Operations. The NSGA-II algorithm uses cross and mutation operations to generate the next generation of individuals. Cross operation generates a new offspring by combining the genes of two parent individuals. Mutation operations increase population diversity by randomly changing certain genes of offspring individuals.

(5) Termination Conditions. The NSGA-II algorithm needs to define appropriate termination conditions. Common termination conditions include reaching the preset maximum number of iterations, reaching the preset time limit, or the algorithm converging to a stable frontier solution. This paper chooses to set the maximum number of iterations (iterations = 300) as the termination condition.

(6) Algorithm Steps. The overall process of the algorithm is shown in Figure 3.

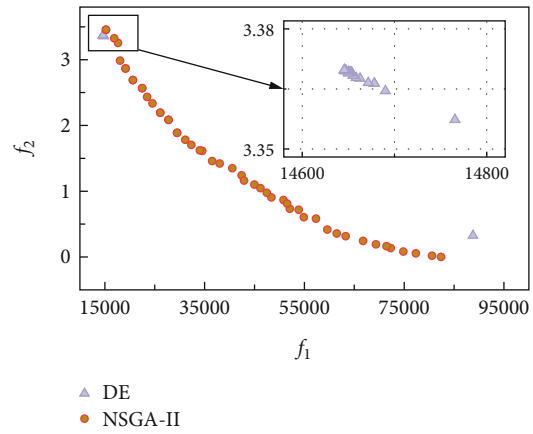

Figure 6: The Pareto frontier point sets under different algorithms.

Step 1. Randomly generate the initial population S_t, where each individual represents a set of solutions, representing the corresponding control quantity at the AGO and COL location, in the format of $[G_1, G_2, G_3, L_1, L_2, L_3]$. Based on the objective function defined earlier, calculate the fitness value of each individual, which is the performance value of the solution on multiple objective functions.

Step 2. Sort the population S_t based on the nondominant relationship between individuals. And calculate the crowding distance for each individual to measure their distribution density in the solution space, which can help maintain the diversity of the population.

Step 3. Perform cross, mutation, and select operations in the genetic operator on the population S_t to obtain the offspring population Q_t. Through this step, it is possible to maintain the diversity of the increased population while retaining outstanding individuals.

Step 4. Merge the parent individual S_t and the offspring individual Q_t to form a new population R_t.

Step 5. Perform nondominated sorting on the new population and assist in crowding ranking based on the hierarchical clustering mechanism. After selecting elite individuals from the population, obtain the new parent population R_{t+1}.

Table 3: The comparison results under different algorithms.

	Initial fault	Over limit line	f_1 after AGO and COL (NSGA-II algorithm)	f_2 before AGO and COL (NSGA-II algorithm)	f_1 after AGO and COL (DE algorithm)	f_2 before AGO and COL (DE algorithm)
The case with the lowest f_1 value	[39, 46]	[8]	15230	3.454502	14645	3.36974
The case with the lowest f_2 value	[39, 46]	[8]	82390	0	88794	0.32574

Step 6. Repeat steps 3 to 5 until the termination condition of the CFB scheme is reached.

The output result is to select the individual with the highest nondominated level from the final population as the optimal solution set for the next analysis or decision-making process.

4. Solution Process of Cascading Failure Blocking Control Model

The process of the ODCF blocking method based on source and load coordinated regulation is shown in Figure 4. Firstly, based on the power grid data, a weighted directed graph with line impedance as the weight is established. Using this graph, the Dijkstra algorithm is used to calculate the three generators and loads closest to the overload line, which are used as the locations for AGO and COL. Based on the operation of the power grid, a multiobjective optimization model is established with the minimum cost of AGO and COL and the minimum LFP as the objective functions. The NSGA-II algorithm is used to solve the Pareto frontier point, and the optimal amount of AGO and COL is calculated according to the actual situation of the power grid, to obtain the optimal scheme for CFB.

5. Example Analysis

5.1. IEEE 39-Bus System Example

5.1.1. Acquisition of Cascading Failure Dataset. The example analysis adopts an IEEE 39-bus system, and Figure 5 shows the IEEE 39-bus system structure diagram. Build a CF model on the MATLAB software platform, use the Matpower toolkit for power flow calculation, use the Dijkstra algorithm to solve the load and generator closest to the overload line, and use the NSGA-II algorithm to solve the optimal amount of AGO and COL.

The compensation prices for unit output changes, unit shutdown compensation prices, and unit interruption load compensation prices of each generator in the system are shown in Tables 1 and 2, referring to the data used in reference [12].

5.1.2. Solving the Cascading Failure Model. According to the solving process of the CFB control model in Section 4, taking the initial fault line [39, 46] as an example, the NSGA-II algorithm and DE (differential evolution) algorithm [26] were used to calculate all optimal solutions that meet the model. The Pareto frontier point sets under different algorithms are shown in Figure 6, and the comparison results under different algorithms are shown in Table 3.

From Figure 6, it can be seen that the Pareto frontier point set distribution of the NSGA-II algorithm is relatively uniform, while the results of the DE algorithm tend to be biased towards two extremes, making it easy to fall into local optima.

From Table 3, it can be seen that when the f_1 value is minimized, the results obtained by the NSGA-II algorithm and the DE algorithm are similar. The DE algorithm yields poorer results compared to the NSGA-II algorithm and cannot explore the optimal solution set. By comparing the computational results of the NSGA-II algorithm and the DE algorithm, it can be seen that the NSGA-II algorithm is more suitable for solving multiobjective problems in this scenario. From the distribution of the Pareto frontier point set, it can be seen that the NSGA-II algorithm can meet the solving needs of this paper.

To verify the rationality of the method proposed in this paper for AGO and COL, taking the initial fault line [39, 46] as an example, the function values under different proportions of AGO and COL capacity are taken as shown in Table 4.

From Table 4, it can be seen that the f_1 value tends to be linear under three conditions: individual AGO, individual COL, and AGO and COL. That is, it increases proportionally with the increase of AGO and COL capacity. This is because under a certain AGO and COL location, the coefficient is the compensation price for AGO and COL which is a certain value. Therefore, the relationship is linear.

In three conditions, the f_2 value is nonlinear, because the relationship between the AGO and COL capacity and the LFP is not a simple linear relationship. In this scenario, the proportional AGO and COL method is most effective in 60% of cases, and the LFP coefficient can reach 4.035114. In the case of individual COL, when the load is reduced to below 20%, the LFP will approach the normal hidden fault probability. In the case of individual AGO, the LFP is displayed as a fluctuating situation, and an unreasonable AGO scheme can actually lead to an increase in the LFP coefficient. The above situation indicates that the AGO and COL problem is not a simple linear problem, and traditional proportional AGO and COL is difficult to achieve the optimal situation.

Taking the minimum values of objective functions f_1 and f_2 as examples, plot the power flow situation and the LFP before and after AGO and COL, as shown in Figure 7.

From Figure 7, it can be seen that after the N-2 fault occurred, the line [8] exceeded the limit, and the LFP

Table 4: Function values under different proportions of AGO and COL capacity.

AGO and COL proportions	f_1	f_2	AGO and COL proportions	f_1	f_2	AGO and COL proportions	f_1	f_2
0% load-0% Gen	256780	6.130336	0% load-100% Gen	156280	0	100% load-0% Gen	100500	8.774853
10% load-10% Gen	231102	5.539328	10% load-100% Gen	140652	0	100% load-10% Gen	90450	9.135659
20% load-20% Gen	205424	4.879771	20% load-100% Gen	125024	0	100% load-20% Gen	80400	12.043879
30% load-30% Gen	179746	4.378068	30% load-100% Gen	109396	0.131257	100% load-30% Gen	70350	20.046128
40% load-40% Gen	154068	4.230895	40% load-100% Gen	93768	0.344691	100% load-40% Gen	60300	9.074085
50% load-50% Gen	128390	4.119907	50% load-100% Gen	78140	0.895001	100% load-50% Gen	50250	6.871781
60% load-60% Gen	102712	4.035114	60% load-100% Gen	62512	1.489316	100% load-60% Gen	40200	7.284503
70% load-70% Gen	77034	4.14629	70% load-100% Gen	46884	2.09822	100% load-70% Gen	30150	14.112022
80% load-80% Gen	51356	4.277807	80% load-100% Gen	31256	2.764133	100% load-80% Gen	20100	35.747854
90% load-90% Gen	25678	4.360522	90% load-100% Gen	15628	3.541157	100% load-90% Gen	10050	5.123711
100% load-100% Gen	0	4.380391	100% load-100% Gen	0	4.380391	100% load-100% Gen	0	4.380391

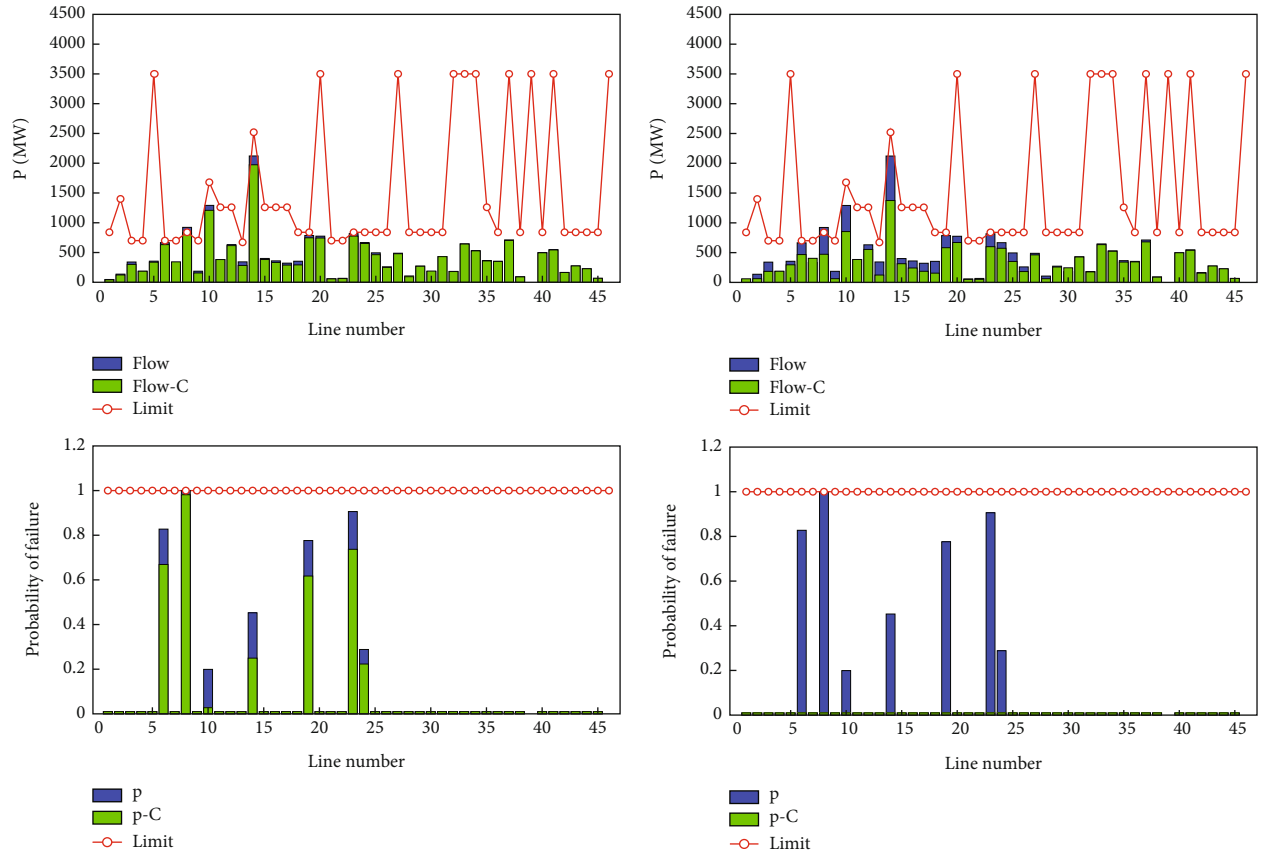

(a) The case with the lowest f_1 value

(b) The case with the lowest f_2 value

Figure 7: Comparison of system status before and after AGO and COL.

reached 1. After the AGO and COL action, the power flow of the out-of-limit line decreased below the limit of the line flow, and the LFP also decreased to the normal level, which can prevent the occurrence of CF. The minimum value of f_1 represents the use of the minimum cost of AGO and COL to reduce the LFP from 1 to below 1, achieving the blocking of CF, suitable for situations that require rapid adjustment. The minimum value of f_2 represents minimizing the failure probability of all lines, which is suitable for situations with multiple adjustable generators and multiple load capacities.

To verify the effectiveness of the proposed method, four scenarios were set up for CF simulation. The top three generators and load nodes in the electrical distance ranking from the fault line were selected as the AGO and COL locations. The comparison data of the grid status before and after AGO and COL are shown in Table 5.

Table 5: Comparison of grid status before and after AGO and COL.

(a) The case with the lowest f_1 value

Initial fault	Over limit line	Cutting machine load capacity	f_1 after AGO and COL	f_2 before AGO and COL	f_2 after AGO and COL
[10, 15]	[9, 19, 23]	[642, 250, 632, 540, 276, 234, 318, 500]	28460	2.9700	2.729085
[33, 46]	[6, 8, 23]	[249, 650, 540, 630, 309, 355, 115, 231, 522]	22740	5.1341	3.659189
[39, 46]	[8]	[647, 250, 540, 368, 319, 522]	15150	4.3804	3.518708
[14, 25]	[3, 6]	[249, 540, 998, 631, 223, 321, 157, 355]	16560	1.9800	1.923736

(b) The case with the lowest f_2 value

Initial fault	Over limit line	Cutting machine load capacity	f_1 after AGO and COL	f_2 before AGO and COL	f_2 after AGO and COL
[10, 15]	[9, 19, 23]	[642, 250, 632, 540, 30, 234, 316, 514]	54080	2.9700	0
[33, 46]	[6, 8, 23]	[249, 627, 540, 629, 50, 155, 9, 231, 520]	89870	5.1341	0
[39, 46]	[8]	[641, 250, 540, 117, 2, 522]	81340	4.3804	0
[14, 25]	[3, 6]	[249, 540, 998, 631, 223, 301, 151, 102]	47450	1.9800	0

Table 6: Comparison of grid status under different quantity of AGO and COL locations.

Initial fault	Top 1 nodes in electrical distance ranking	f_2	Top 2 nodes in electrical distance ranking	f_2	Top 3 nodes in electrical distance ranking	f_2	Top 4 nodes in electrical distance ranking	f_2
[8, 14]	[15][15]	1.185156	[15, 19] [15, 19]	0.849173	[15, 19, 113] [15, 19, 17]	0.838978	[15, 19, 113, 18] [15, 19, 17, 113]	0.839903
[89, 94]	[61][60]	0.326329	[61, 62] [60, 62]	0.326329	[61, 62, 65] [60, 62, 116]	0	[61, 62, 65, 116] [60, 62, 116, 59]	0
[31, 122]	[25][23]	0.220808	[25, 26] [23, 24]	0.1363	[25, 26, 24] [23, 24, 17]	0.111237	[25, 26, 24, 27] [23, 24, 17, 27]	0
[38, 76]	[24, 25][23]	0.173136	[24, 25, 26] [23, 24]	0	[24, 25, 26, 32] [23, 24, 32, 17]	0	[24, 25, 26, 32, 27] [23, 24, 32, 17, 22, 27]	0

From Table 5, it can be seen that whether it is the minimum value of objective function f_1 or the minimum value of f_2, the power flow of the out-of-limit line is effectively alleviated after the CFB method proposed in this paper is used to AGO and COL.

Based on Tables 4 and 5, it can be seen that under the condition of individual COL, when the 30% load is 100% of the generator, the AGO and COL cost is 109396, and the LFP coefficient is 0.131257. In the case of individual AGO, an unreasonable AGO scheme leads to further deterioration of the power flow situation of the line, and the LFP coefficient is all higher than 4.380391. By using the method proposed in this paper, the LFP coefficient can be achieved to be 0 at a AGO and COL cost of 89870. Prove that the combination of AGO and COL is more effective than individual AGO or individual COL. The method proposed in this paper is more effective than the traditional proportional cutting method.

5.2. IEEE 118-Bus System Example

5.2.1. Selection of AGO and COL Location. To verify the adaptability of the method proposed in this article, a more complex IEEE 118-bus system was used for verification. Set the initial fault as an N-2 fault, select four scenarios for fault simulation, and set different numbers of AGO and COL locations for simulation. The simulation results are shown in Table 6.

Table 6 shows the LFP coefficients under the minimum f_2 value. It can be seen from the table that as the number of nodes selected for AGO and COL increases, the LFP coefficients will also decrease. This is because as the number of selectable nodes increases, the number of schemes for CFB also increases. In practical application scenarios, it is necessary to consider whether the generator units and loads that need to be adjusted have adjustable conditions.

5.2.2. Calculation of AGO and COL Capacity. According to the solving process of the CFB control model in Section 3, use the NSGA-II algorithm to calculate all optimal solutions that comply with the AGO and COL model. To verify the effectiveness of the proposed method, four scenarios were set up for CF simulation. The comparison data of the grid status before and after AGO and COL are shown in Table 7.

From Table 7, it can be seen that whether it is the minimum value of objective function f_1 or the minimum value

Table 7: Comparison of grid status before and after AGO and COL.

(a) The case with the lowest f_1 value

Initial fault	Over limit line	Cutting machine load capacity	f_1 after AGO and COL	f_2 before AGO and COL	f_2 after AGO and COL
[8, 14]	[21]	[0, 0, 0, 61, 44, 11]	2340	2.0439	1.907978
[89, 94]	[90]	[153, 0, 388, 67, 77, 184]	1323	1.6296	1.635127
[31, 122]	[33]	[178, 314, 0, 7, 13, 11]	1512	0.9900	0.985472
[38, 76]	[31, 33]	[0, 150, 314, 0, 7, 13, 59, 11]	2520	1.9800	1.575194

(b) The case with the lowest f_2 value

Initial fault	Over limit line	Cutting machine load capacity	f_1 after AGO and COL	f_2 before AGO and COL	f_2 after AGO and COL
[8, 14]	[21]	[0, 0, 0, 0, 0, 1]	11010	2.0439	0.839903
[89, 94]	[90]	[1, 0, 215, 24, 77, 184]	14229	1.6296	0.000000
[31, 122]	[33]	[13, 314, 0, 0, 1, 1]	9827	0.9900	0.111237
[38, 76]	[31, 33]	[0, 0, 284, 0, 7, 13, 56, 11]	9327	1.9800	0.000000

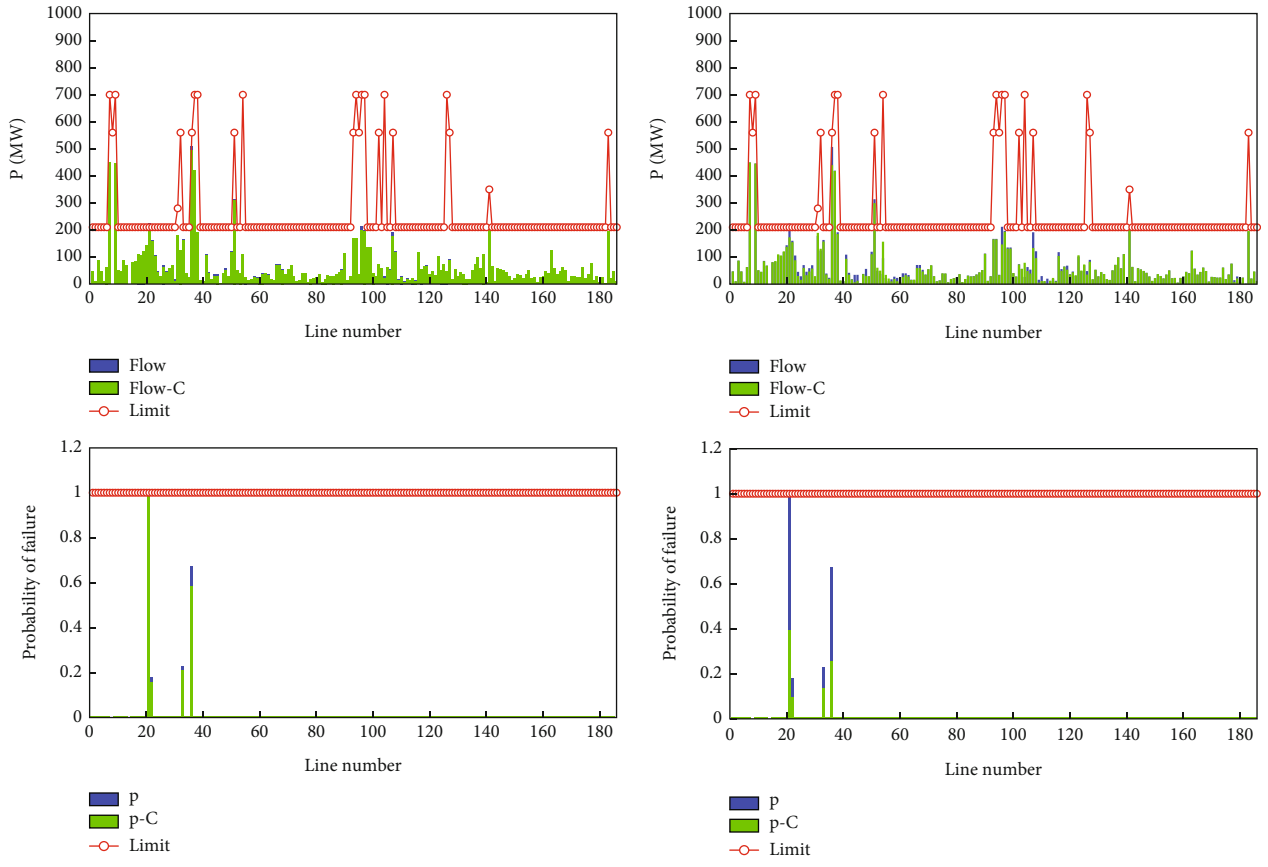

(a) The case with the lowest f_1 value

(b) The case with the lowest f_2 value

Figure 8: Comparison of system status before and after AGO and COL.

of objective function f_2, the power flow of the overload line is effectively alleviated after the CFB method proposed in this paper is used for AGO and COL.

Taking the initial fault line [8, 14] as an example, plot the power flow situation and LFP before and after AGO and COL, as shown in Figure 8.

From Figure 8, it can be seen that after the N-2 fault occurred, the line [21] exceeded the limit, and the LFP reached 1. After conducting AGO and COL, the power flow of the overloaded line [21] decreased below the line power flow limit, and the LFP also decreased to normal levels. The failure probability of other high failure probability lines

has decreased to varying degrees. The method proposed in this paper is equally applicable in more complex systems.

6. Conclusion

To suppress large-scale power outages caused by ODCF, this paper proposes a blocking method for ODCF in the power grid based on source and load collaborative regulation. This method utilizes graph theory and intelligent optimization algorithms to solve the CF model by exploring the relationship between the load and generator and the overload lines and obtains the ODCF blocking scheme. Its effectiveness and feasibility are verified through the IEEE 39-bus system and IEEE 118-bus system. The main conclusions are as follows:

(1) This paper analyzes the development process of CF and proposes to block the occurrence of CF through AGO and COL. Based on this, a blocking method for ODCF based on source and load collaborative regulation is designed. A solution method for the ODCF blocking model was proposed, and the model solving process was established. It is proposed to select the AGO and COL locations and calculate the AGO and COL capacity in sequence. This method simplified the solving process and greatly reduced the computational workload

(2) Compared with the traditional proportional cutting method, the method proposed in this paper has better results and can make the LFP coefficient closer to normal at a lower compensation price, effectively alleviating the phenomenon of line overload and blocking the continuation of ODCF

(3) By comparing the power grid situation under different numbers of AGO and COL locations, it can be seen that as more nodes are selected for AGO and COL, the number of schemes for blocking CF also increases, which can make the LFP coefficient closer to normal conditions

This paper equates the ODCF blocking problem to a multiobjective optimization problem, which can accurately reflect the results of current level blocking. However, the equivalence of cascading failures propagation process is not involved, and future research can focus on it.

Nomenclature

CF: Cascading failures
CFB: Cascading failure blocking
AGO: Adjusting generator output
COL: Cutting off load
ODCF: Overload-dominant cascading failures
LFP: Line failure probability
N: The set of all nodes $n_0, n_1, \cdots n_n$ in the weighted directed graph
E: The set of all edges $e_0, e_1, \cdots e_n$ in the weighted directed graph
W: The weight set of all edges $w_0, w_1, \cdots, w_n$ in the weighted directed graph
a_{ij}: The length between nodes n_i and n_j
N_G: The number of switchable generator nodes
N_L: The number of load shedding nodes
$c_{G,i}$: The cutting cost of the i-th generator node
$c_{L,j}$: The cutting cost of the j-th load node
$\Delta P_{G,i}$: The adjustment amount of the i-th generator node
$\Delta P_{L,j}$: The load shedding amount of the j-th load node
p_n: The line failure probability
p_0: The probability of hidden faults on the line
P: The transmission power of the line
P_m: The upper limit of line transmission power
b: The multiple of the maximum transmission power
N_l: The number of lines
N_{ol}: The number of lines cut off due to faults
$Q_{L,ik}$: The reactive power of the corresponding controllable load generated when $P_{L,ik}$ is cut off
U_i^l: The voltage amplitude of the i-th node during the accident state
P_{Li}, Q_{Li}: The active and reactive power of the i-th node load
G_{ij}, B_{ij}: The element of the node admittance matrix
θ_{ij}^l: The angle difference between nodes i and j
$P_{Gi,\max}$, $P_{Gi,\min}$: The upper and lower limits of the active output of the i-th generator
$Q_{Gi,\max}$, $Q_{Gi,\min}$: The upper and lower limits of the reactive power output of the i-th generator
P_{ij}^l: The transmission power of the line ij during the accident state
$P_{ij,\max}$: The maximum allowable transmission power of line ij
$U_{i,\max}$, $U_{i,\min}$: The upper and lower limits of voltage amplitude at node i.

Data Availability

The data are available from the corresponding author upon reasonable request.

Conflicts of Interest

On behalf of all the authors, the corresponding author states that there is no conflict of interest.

Acknowledgments

A tribute to everyone who contributed to the writing of the paper is at the end of the paper. First of all, I would like to thank Xi'an University of Technology for providing the scientific research platform. Second, thanks are due to the National Natural Science Foundation of China (52077176) for the financial support of this paper. Finally, I would like to thank Prof. Liu for his guidance through each stage of

the process, Yue Liu for her help in the writing of the paper, Chenjing Li for her help in the data processing, and Professor Zhi for her help in the modification of the diagram.

References

[1] M. Z. Zakariya and J. Teh, "A systematic review on cascading failures models in renewable power systems with dynamics perspective and protections modeling," *Electric Power Systems Research*, vol. 214, no. B, article 108928, 2023.

[2] X. Zhang, L. Dong, T. Haicheng, and C. K. Tse, "An integrated modeling framework for cascading failure study and robustness assessment of cyber-coupled power grids," *Reliability Engineering & System Safety*, vol. 226, article 108654, 2022.

[3] J. Zhou, D. W. Coit, F. A. Felder, and S. Tsianikas, "Combined optimization of system reliability improvement and resilience with mixed cascading failures in dependent network systems," *Reliability Engineering & System Safety*, vol. 237, article 109376, 2023.

[4] J. Hou, Q. Zhai, and X. Guan, "Fast prediction and avoidance of cascading line failures based on ANN with feedbacks," *International Journal of Electrical Power & Energy Systems*, vol. 145, article 108655, 2023.

[5] M. Salama, W. El-Dakhakhni, and M. Tait, "Systemic risk mitigation strategy for power grid cascade failures using constrained spectral clustering," *International Journal of Critical Infrastructure Protection*, vol. 42, article 100622, 2023.

[6] S. Gharebaghi, N. R. Chaudhuri, T. He, and T. La Porta, "An approach for fast cascading failure simulation in dynamic models of power systems," *Applied Energy*, vol. 332, article 120534, 2023.

[7] W. Lin, Y. Jun, Q. Guo, Z. Wang, J. Qi, and F. Yu, "Analysis on blackout in Argentine power grid on June 16, 2019 and its enlightenment to power grid in China," *Proceedings of the Chinese Society of Electrical Engineering*, vol. 40, no. 9, pp. 2835–2841, 2020.

[8] Z. Jinfeng, C. Xiaodan, J. Xu, L. Ming, L. Xuan, and F. Xue, "An optimization method of load-shedding strategy based on a multi-user non-cooperative game model," *Power System Protection and Control*, vol. 48, no. 22, pp. 127–134, 2020.

[9] Y. Wang, Z. Lu, L. Qiang, and Y. Jingbo, "Optimal control algorithm for static safety correction of power grid based on source and load coordination," *Power System Protection and Control*, vol. 47, no. 20, pp. 73–80, 2019.

[10] Y. Xu, Z. Jing, and F. Shitong, "Line overload emergency control based on power sensitivity and minimized economic compensation," *Electric Power Automation Equipment*, vol. 37, no. 1, pp. 118–123, 2017.

[11] Y. Zhao, B. Cai, H. H.-S. Kang, and Y. Liu, "Cascading failure analysis of multistate loading dependent systems with application in an overloading piping network," *Reliability Engineering & System Safety*, vol. 231, article 109007, 2023.

[12] S. Mao, J. Yanbing, and Z. Qi, "Research on emergency control method considering severity of overheating of overload line," *Power System Protection and Control*, vol. 47, no. 16, pp. 34–42, 2019.

[13] G. Guoxiao, G. Guangchao, B. Gao, Z. Wuzhi, J. Quanyuan, and H. Daoshan, "Blocking control of power system cascading failures considering line outages probability," *Power System Technology*, vol. 44, no. 1, pp. 266–272, 2020.

[14] L. Yumeng, G. Xueping, and T. Wang, "Multi-stage blocking control of power system cascading failures considering propagation path," *Electric Power Automation Equipment*, vol. 41, no. 12, pp. 151–157, 2021.

[15] K. Yongchao, K. Liao, L. Bo, J. Yang, and Z. He, "Line overload control strategy based on bi-level optimization programming," *Electric Power Automation Equipment*, vol. 41, no. 12, pp. 158–165, 2021.

[16] S. Yang, W. Chen, X. Zhang, and Y. Jiang, "Blocking cascading failures with optimal corrective transmission switching considering available correction time," *International Journal of Electrical Power & Energy Systems*, vol. 141, article 108248, 2022.

[17] Z. Jingjing, Y. Yang, D. Ming, Q. Yucheng, and T. Luo, "Control strategy for cascading overload considering prim partition and generation adjustment," *High Voltage Engineering*, vol. 43, no. 11, pp. 3675–3682, 2017.

[18] M. Fekri, J. Nikoukar, and G. B. Gharehpetian, "Vulnerability risk assessment of electrical energy transmission systems with the approach of identifying the initial events of cascading failures," *Electric Power Systems Research*, vol. 220, article 109271, 2023.

[19] D. Ming, Q. Yucheng, and Z. Jingjing, "Multi-timescale cascading failure evolution and risk assessment model," *Proceedings of the Chinese Society of Electrical Engineering*, vol. 37, no. 20, pp. 5902–5912, 2017.

[20] M. Noebels, I. Dobson, and M. Panteli, "Observed acceleration of cascading outages," *IEEE Transactions on Power Systems*, vol. 36, no. 4, pp. 3821–3824, 2021.

[21] H. Ebrahimi, M. Abapour, B. Mohammadi-Ivatloo, S. Golshannavaz, and A. Yazdaninejadi, "Decentralized approach for security enhancement of wind-integrated energy systems coordinated with energy storages," *International Journal of Energy Research*, vol. 46, no. 4, pp. 5006–5027, 2022.

[22] K. Bio Gassi and M. Baysal, "Analysis of a linear programming-based decision-making model for microgrid energy management systems with renewable sources," *International Journal of Energy Research*, vol. 46, no. 6, pp. 7495–7518, 2022.

[23] K. P. Schneider, X. Sun, and F. Tuffner, "Adaptive load shedding as part of primary frequency response to support networked microgrid operations," *IEEE Transactions on Power Systems*, vol. 39, no. 1, pp. 287–298, 2024.

[24] X. Liang, H. Yang, B. Xue et al., "An identification method for dangerous lines under power flow transfer in a distribution network open circuit," *Power System Protection and Control*, vol. 49, no. 23, pp. 11–17, 2021.

[25] M. Z. Islam, S. N. Edib, V. M. Vokkarane, Y. Lin, and X. Fan, "A scalable PDC placement technique for fast and resilient monitoring of large power grids," *IEEE Transactions on Control of Network Systems*, vol. 10, no. 4, pp. 1770–1782, 2023.

[26] O. T. Amusan, N. I. Nwulu, and S. L. Gbadamosi, "Identification of weak buses for optimal load shedding using differential evolution," *Sustainability.*, vol. 14, no. 6, p. 3146, 2022.